Application of the Modified Biochar from Sewage Sludge for Removal of Pb(II) from Aqueous Solution: Kinetics, Equilibrium and Thermodynamic Studies

Zhang, Lequn•

Key Laboratory of Western China' s Environmental System, Ministry of Education, College of Resource and Environment, Lanzhou University, Lanzhou 730000, Gansu, P.R. CHINA

Yu, Tao

School of Petrochemical Engineering, Lanzhou University of Technology, Lanzhou 730050, Gansu, P.R. CHINA

Nan, Zhongren

Key Laboratory of Western China' s Environmental System, Ministry of Education, College of Resource and Environment, Lanzhou University, Lanzhou 730000, Gansu, P.R. CHINA

Wu, Zhenjun; Li, Bin; Li, Shunyi*+

School of Chemical Engineering and Energy, Zhengzhou University, Zhengzhou 450001, Henan, P.R. CHINA

ABSTRACT: *An adsorbent Modified Biochar (MB) made from sewage sludge was characterized by FT-IR spectra and SEM image. The effects of contact time, solution temperature, pH and initial concentration on the adsorption performance Pb(II) onto MB was investigated in a batch adsorption experiment. Results showed that MB had great adsorption capacity, due to the existence of hydroxyl, carboxyl, ether, alcohol and amino groups. As the contact time prolonged, the adsorption quantity of MB increased sharply first and then tended to the balance. The adsorption capacity increased slightly with the temperature increase. The effect of pH on the absorbability of MB was non-linear, and the maximum adsorption capacity was obtained when the pH was approximately 6. The adsorption capacity increased abruptly first and then become slowly with the initial concentration increase. Compared with the pseudo-first-order, the pseudo-second-order kinetic models were more suitable to test the kinetic experimental data. Equilibrium data were analyzed using the Langmuir and Freundlich isotherm models and it was found to correspond to the Langmuir isotherm model better.*

KEYWORDS: *Pb(II); Modified biochar; Adsorption kinetics; Adsorption isotherms; Adsorption mechanism.*

INTRODUCTION

Water pollution caused by heavy metals has become a serious environmental and public health issue for a long time. The most common heavy metals are lead, zinc, copper, etc. [1]. Lots of literature show that lead is a toxic heavy metal and is a dangerous contaminant in the aqueous environment [2,3]. Drinking those containing lead ions, even in very low concentration, would lead to various spectrum health problems, such as protein degeneration, tissue erosion, and paralysis of the central nervous system [4,5]. Lead ions are mainly introduced into natural water by a variety of industrial wastewater such as coating, automotive, aeronautical and steel industries. Considering the lead ions accumulating in plants and animals easily, it is necessary to purify lead ions from wastewater before use.

Various technologies have been employed for the removal of Pb(II) ions including coagulation, flocculation, ion exchange, membrane separation, oxidation, etc. [6]. But these methods often have drawbacks such as large sludge production, high cost, technical constraints, etc. [2]. Compared with the methods mentioned above, the adsorption method was widely applied in the water treatment, for the advantages of low operating cost, simple design, high efficiency and minimum generation of toxic sludge [7, 8]. Activated carbon is widely used as an adsorbent for its better adsorption ability, and the adsorption of organics and metal contaminants by activated carbon has been widely investigated [9,10]. The high cost makes it less economically viable as an adsorbent. Therefore, it is necessary to explore a low cost and high-efficiency adsorbent [8].

Biochar is classified as a promising adsorbent for the removal of Pb(II) ions in high efficiency, because of its low cost and high adsorption capacity, as a natural material. In addition, biochar gained considerable interests mainly because of their high degree of porosity and extensive surface area, along with abundant organic functional groups and mineral oxides [11-14]. Meanwhile, it also provides a method for the treatment of sewage sludge, which could pose a big environmental burden for the authorities. An increasing number of studies were focused on synthetic feed models made from different organic materials and evaluated the adsorption performance. However, only a few of them have assessed the performance of biochar made from sewage sludge and conducted the relevant equilibrium and kinetic studies [10, 15].

The research is mainly focused on the biosorption of Pb(II) ions with Modified Biochar (MB) and takes the biosorption kinetics and equilibrium into account. Additionally, the possible functional groups present on the surface of MB and the mechanism involved in lead biosorption were characterized by FT-IR and SEM analysis.

EXPERIMENTAL SECTION

Preparation of the modified biochar

The raw material for manufacturing biochar was Sewage Sludge (SS), which (moisture content of 80%) was obtained from the condensing tank of a paper mill located in Luohe (Henan Province, China). Firstly, SS was washed with double distilled water to remove dirt and other particulate matters, and then the SS was dried at 100°C for 3 h until there was no water vapor released. Finally, biochar was made after the pyrolysis of SS at 650°C for 6 h.

The modified process of biochar obtained above was as follows: (1) homogenize and sieve the biochar to the desired size (0.85~1.00 mm); (2) select 1 g powdered biochar randomly and put them in a 250 mL flask with 50 ml H_2SO_4 solution (3 mol·L^{-1}); (3) shake the flask on a THZ-82 constant temperature shaker at 25°C for 6 h; (4) take the biochar out and wash them with double distilled water until the wash water became neutral. Finally, the prepared Modified Biochar (MB) was stored in a desiccator. It is worth noting that the modified biochar was not sieved before using in the experiments.

Analytical methods

The initial and final concentrations of Pb(II) in the adsorption experiments were measured with Flame Atomic Absorption Spectrophotometer (FAAS). Infrared spectra (400 ~ 4000 cm^{-1}) of both MB and Pb(II)-MB were recorded by a WQF-510 FT-IR spectrometer and the data were analyzed using the software of Main FTOS. The surface structure of the MB before and after adsorption was analyzed by scanning electron microscopy (SEM JSM-7500Japan). SEM images were obtained at 10.0 kV on a scanning electron microscope after being coated with gold. The specific surface area and pore volume of the MB were analyzed with a NOVA4200e surface area analyzer.

Experimental design

(1) Effect of contact time. To observe the effect of contact time on the adsorption capacity, a series of 10 mg of MB were placed in a certain number of 100 ml flasks, 50 mL Pb(II) solution was added to each flask (initial concentrations of 90 mg/L), then the flasks were shaken with the speed of 125 rpm in a constant temperature shaker at 25°C. The flask was taken at appropriate intervals, such as 10 min, 20 min, 30 min, 1 h, 1.5 h, 2.5 h, 3 h, 3.5 h, and 4 h, and the residual concentration of Pb(II) was measured by FAAS. The adsorption capacity of Pb(II) was calculated as the following equation [16].

$$q_t = V \times (C_0 - C_t) / W \qquad (1)$$

where q_t is the adsorption quantity of Pb(II) at the equilibrium condition; V is the volume of Pb(II) solution; C_0 is the initial concentration of Pb(II), mg/L; C_t (mg/L) is the equilibrium concentration of Pb(II) after adsorption, mg/L; and W is the weight of the MB added to the flasks.

(2) Effect of initial solution pH. To study the effect of solution pH, the pH of the Pb(II) solutions (initial concentration is 90 mg/L) were adjusted to 3.0, 4.0, 5.0, 5.5, 6.0, 6.3, 7.0, 8.0, 9.0, 10.0, 11.0, 12.0 with 0.1 mol·L^{-1} HNO$_3$ and 0.1 mol/L NaOH solutions, which were measured using a digital pH meter (pHS-3C). A series of MB samples (10 mg) were added into 50 mL Pb(II) solution with different pH designed above and shaken for 4 h at 125 rpm in a constant temperature shaker at 25°C. Selecting 4 h as the experimental time because the maximum setup time of the shaker used was 240 min.

(3) Effect of solution temperature. To study the effect of solution temperature, 10 mg modified biochar was added into a series of 50 ml Pb(II) solution, and the initial pH of each solution was adjusted to 6.0. Then the flasks were shaken while keeping the temperature at 25°C, 35°C and 45°C, respectively, for 4 h with the speed of 125 rpm in a thermostatic reciprocating shaker. The residual concentration of Pb(II) ions was determined according to the method described above.

(4) Effect of initial adsorbate concentration. For equilibrium adsorption experiments, 50 mL of various initial concentrations (range from 20 to 200 mg/L) of Pb(II) solution was mixed with 10 mg MB, and the initial pH of each solution was adjusted to 6.0. The solutions were shaken at 25°C, 35°C and 45°C, respectively, until equilibrium was established. Finally, the residual concentration of Pb(II) ions was measured by FAAS.

Adsorption kinetics

In order to investigate the controlling mechanism of adsorption processes, experimental data obtained from the effect of contact time Section were used to conduct the fowling adsorption kinetics.

(1) Pseudo-first-order model. This model developed by Langeren assumed that the adsorption rate decreased linearly as the adsorption capacity increased [17]. The pseudo-first order model was given as Eq. (2).

$$\ln(q_e - q_t) = \ln q_e - k_1 t \qquad (2)$$

Where q_e and q_t are the adsorption quantities of Pb(II) at the equilibrium and that at a certain time t (min), respectively, mg/g; k_1 is the pseudo-first-order rate constant, min^{-1}.

(2) Pseudo-second-order model. This model assumed that the rate-limiting step was the interaction between two reagent particles [17, 18]. The linear form of the pseudo-second-order kinetic model was given as Eq. (3).

$$t / q_t = 1 / (k_2 q_e^2) + t / q_e \qquad (3)$$

Where k_2 is the pseudo-second-order rate constant, g·/(mg·min)

Adsorption isotherms

The adsorption isotherm is used to explain the interaction of the adsorbate ions with the adsorbent. In order to describe the adsorption process and provide better comprehension of the mechanism of Pb(II) onto MB, a series of adsorption tests of MB (10 mg) with different initial concentrations (4~114 mg/L) of Pb(II) solution (50 ml, pH=6) at different temperatures (30°C, 40°C, 50°C). The experimental data were simulated by both the Langmuir and Freundlich isotherm models. The Langmuir isotherm is the theoretical model for identical adsorption heat and monolayer adsorption, which was given as Eq. (4) [19].

$$q_e = K_L C_e q_m / (1 + K_L C_e) \qquad (4)$$

Where K_L *is* the Langmuir isotherm constant, L/mg; C_e is the equilibrium concentration of Pb(II) in solution, mg/L; q_m is the maximum adsorption value, mg/g.

The linear form of Eq. (4) was shown in Eq. (5), which could be employed to determine the q_m and K_L values from the angular and linear coefficents obtained by plotting C_e/q_e as a function of C_e.

$$C_e / q_e = 1/K_L q_m + C_e / q_m \qquad (5)$$

The Freundlich isotherm is shown in Eq. (6) is an empirical equation, which is used to describe adsorption at multilayers and adsorption on a heterogeneous surface.

$$q_e = K_F C_e^{1/n} \qquad (6)$$

Eq. (6) can also be expressed in the linearized logarithmic form as Eq. (7).

$$\ln q_e = \ln K_F + 1/(n \ln C_e) \qquad (7)$$

Where K_F and n are Freundlich isotherm constants related to the adsorption capacity and intensity of the sorbent, respectively.

RESULTS AND DISCUSSION
Characterization of FT-IR, SEM

FT-IR spectroscopy was performed to assess the chemical functional groups on MB and the Pb(II)-loaded MB. The absorbance data were obtained for wave numbers in the range of $400\sim4000$ cm^{-1} and analyzed using software Main FTOS. The infrared spectra of MB and the Pb(II)-loaded MB are shown in Fig. 1. Clearly, there were small but evident peaks (marked in Fig. 1) at bands of 3616 cm^{-1} and 3571 cm^{-1}, respectively, for FT-IR spectra of MB, while that of Pb(II)-loaded MB did not show any obviously peaks within these bands. The peaks at 3616 cm^{-1} and 3571 cm^{-1} in MB is assigned to the stretching vibration of -O-H in the alcohol group [20-21], the disappearance of these peaks in Pb(II)-loaded MB indicating the coordination of Pb(II) ions with alcoholic hydroxyl functional groups. The band in the MB located at 1623 cm^{-1} is associated with -COO- (carboxylic groups) stretching vibration, however, it was disappeared after reacted with Pb(II) ions, confirming the coordination between Pb^{2+} and -COO- (carboxylic groups). The shifts of the band at 1156 cm^{-1} to 1090 cm^{-1} and 1095 cm^{-1} to 1050 cm^{-1} indicate the C-O stretching of ether groups alcoholic groups [22], which suggests the complexation
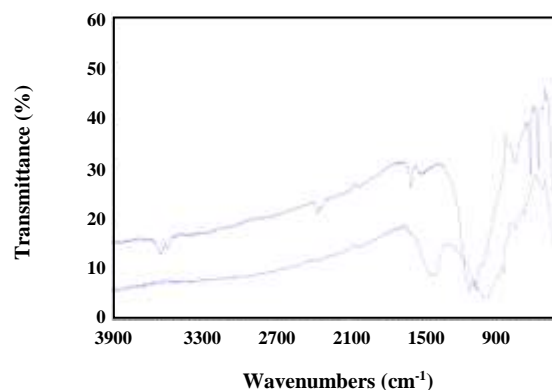

Fig. 1: FT-IR spectra of MB and Pb(II)-loaded MB.

between Pb(II) ions and ether groups, alcoholic groups. The band at 796 cm^{-1} can be attributed to -NH$_2$ stretching vibration, which shifted to 780 cm^{-1} after Pb(II) ions adsorption, indicating coordination of Pb^{2+} with -NH$_2$. A strong peak appearing at 667 cm^{-1} and 602 cm^{-1} were caused by hydroxyl groups. However, the disappearance of the spectrum may be attributed to the complexation between Pb^{2+} and hydroxyl groups. These results indicated that the adsorption of Pb(II) onto MB could be attributed to the hydroxyl reactive groups, carboxylic groups (-COO-), ether groups, alcoholic groups, and amino groups.

The electron micrographs of MB before and after Pb(II) ions adsorption were shown in Fig. 2. The surface characterization showed that MB had a relatively high surface area1800 m^2/g (measured with N$_2$). The surface area gives an indication of the extent of porosity as highly porous structures, especially microporous structures, have a high surface area. It should be highlighted that MB had a tight and porous structure, which is beneficial for the adsorption process. In this sense, we can speculate that the adsorption of Pb(II) onto MB could occur by pore-penetration. However, after adsorption, many large pores in a honeycomb shape were shaped on the surface of MB, interspersed with generally large pores may be due to the reaction with Pb(II) [23].

Effect of contact time and temperature

Fig. 3 shows the variation trend of adsorption quantities of Pb(II) with MB during different adsorption time. Clearly, adsorption time has significant effects on the adsorption quantity. As shown in Figure e, MB had an almost constant adsorption rate in the first 60 min.
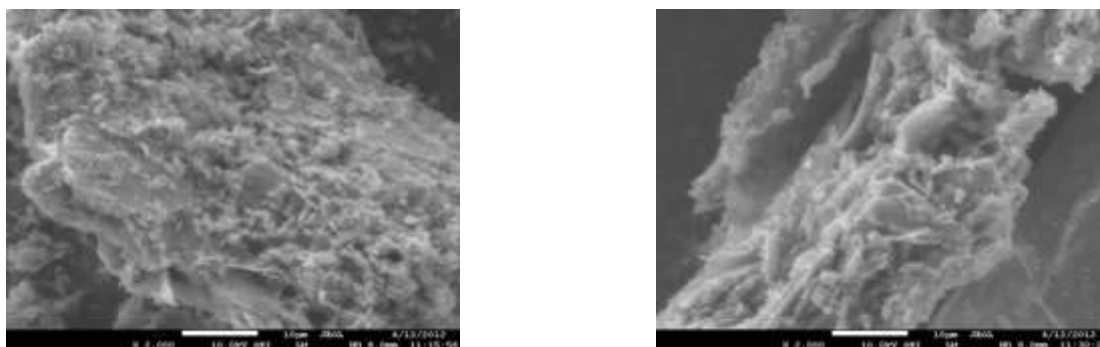
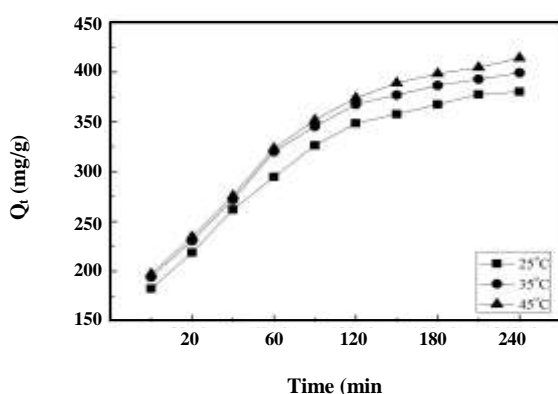*Fig. 2: SEM images of MB before (a) and after (b) Pb(II) ions adsorption.*

Fig. 3: Effect of contact time and temperature on the uptake of Pb(II) ions by MB at pH= 6 and the initial concentration of Pb(II) ions is 90 mg/L.

Speculation was that the adsorption of MB was physical adsorption at the beginning and Pb(II) ions were mainly adsorbed onto the surface of MB. In addition, the concentration gradient of Pb(II) between the solution and the MB surface was big enough, leading to the constant and big adsorption rate. As time prolonging, Pb(II) ions spread to the internal pore of MB and reacted with the activity groups slowly, thus the adsorption rates slowed down. When the test time reached to 4 h, the adsorption rates at different temperatures have a further decline. Fig. 3 shows that the maximum adsorption quantities could reach $380 \sim 414$ mg/g, which was 15 times to G. Blázquez [2] and 10 times to Jyotikusum Acharya [23]. Therefore, it could be considered that the adsorption could gradually achieve a balance after 4 h.

Fig. 3 also compared the adsorption quantities of MB at different solution temperatures. The results show that the adsorption rate shows an upward trend with the temperature increase, proving that the adsorption of MB to Pb(II) is an endothermic process. The maximum adsorption capacity of MB at 25°C, 35°C and 45°C were 380, 399 and 414 mg/g, respectively, which illustrates that temperature has a slight impact on the adsorption capacity of Pb(II), too.

Effect of pH

The pH value is an important parameter that influences the adsorption of Pb(II) with MB. As shown in Fig. 4, the adsorption capacity of MB showed a slight increase with pH increasing from 3 to 5. When the pH value continued to increase, the adsorption capacity increased significantly and then decreased abruptly, and the maximum adsorption occurred when pH=6. Interestingly, the adsorption capacity of MB for Pb(II) was near to zero in the pH range of $7 \sim 10$ and the values could maintain $300 \sim 400$ mg/g when the pH attained to11-12. The main reasons can be explained as follows: The pH dependence of metal adsorption can largely be related to the type and ionic state of the functional groups of the adsorbent surface, Pb(II) ions present in the forms of Pb^{2+}, $Pb(OH)^+$, $Pb(OH)_2^0$ and $Pb(OH)_3^-$ at different pH values. When the pH<5.0, the main ions form is Pb(II) ions and it is mainly removed by adsorption reaction or ion exchange between Pb(II) ions or other heavy metal (Ca^{2+}, Mg^{2+}) and the ion exchange sites on the surface. At the acid condition (pH<5.0), the H^+ concentration is high, which can cause competition with Pb(II) ions for surface adsorption sites and result in a decrease in adsorption of Pb^{2+} ions. Therefore, the adsorption capacity of MB will become larger with the pH value increase in the range of $3 \sim 5$.
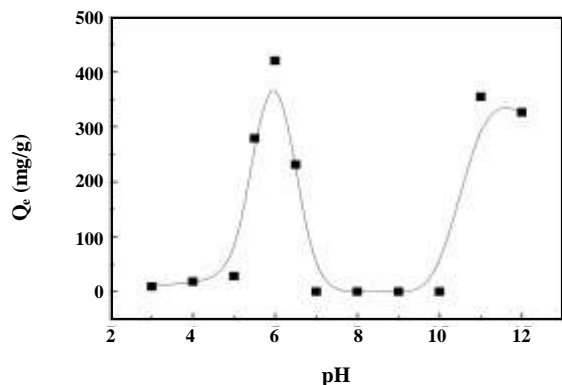
Fig. 4: Effect of pH on the uptake of Pb(II) at different pH values (3-12).

Fig. 5: Effect of initial concentration on the uptake of Pb(II) at different concentration (20 mg/L - 200 mg/L; pH=6).

The ions exist at pH 5~7 are mainly $Pb(OH)^+$, which are easy to be adsorbed on the negatively charged biochar surface (pKa=1.2×10^{-15}). The quantity of $Pb(OH)^+$ converted from the other Pb(II) forms might be easier when the pH was in the range of 5 ~ 7, leading to the removal of Pb(II) maintains a high level and reaches the maximum. In the range of pH 7~10, the main species of Pb(II) is $Pb(OH)_2^0$, which is mainly removed by physical adsorption, thus the adsorption capacity was maintained at a low level. MB has a high adsorption capacity when the pH > 10 was mainly because most Pb(II) ions were transferred to $Pb(OH)_3^-$, which was easily absorbed. There was a slight decrease of Pb(II) adsorption on MB when the pH increased from 11 to 12, which was contributed partly to the competition between –OH and $Pb(OH)_3^-$ [24].

Effect of initial concentration

The initial concentration of the adsorbate plays an important role in the adsorption process. The adsorption of Pb(II) onto MB at different initial concentrations when pH=6 was studied and the results were shown in Fig. 5. It was shown that higher initial Pb(II) concentration led to an increase in adsorption capacity, the adsorption capacity of Pb(II) ions onto MB increased abruptly in the initial concentration range (from 20 mg/L to 80 mg/L) from 123 to 326 mg/g. Compared with the results above, when the initial Pb(II) concentration increased from 80 to 160 mg/L, the Pb(II) adsorption capacity increased slowly from 355 to 488 mg/g. This may be attributed to the concentration gradient developed between the Pb(II) solution and the surface of the MB. The higher initial
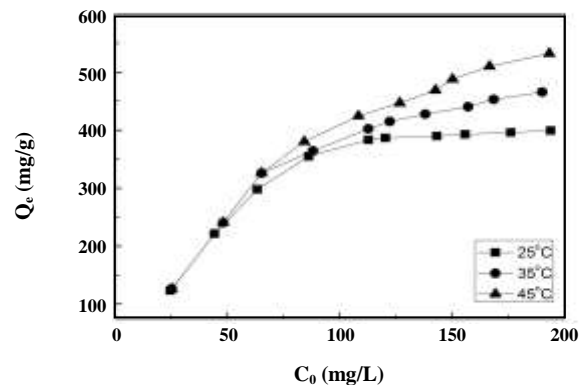
Pb(II) concentration leading to faster and more strongly binding sites compared to lower concentrations of Pb(II) at the same dose of adsorbent. However, when the initial Pb(II) concentration was attained to more than 80 mg/L, the increase rate was smaller than in the concentration range from 20 to 80 mg/L. When the initial Pb(II) concentration was more than 160 mg/L, the complete adsorption equilibrium was obtained at 25°C. Though the adsorption at 35°C and 45°C did not reach equilibrium, the maximum adsorption capacity changed slightly. This can be expressed that in the initial stage, there was enough MB exterior surface and active site for the Pb(II) to be adsorbed, once the exterior surface reached saturation, the Pb(II) ions penetrated through the pores and were adsorbed inside them until adsorption equilibrium [25, 26].

Adsorption kinetics

In order to investigate the controlling mechanism of adsorption processes on the MB, the pseudo-first-order and pseudo-second-order equations were used to model the kinetics of lead adsorption based on the adsorption quantities changes per time interval in series of Pb(II) solutions with an initial concentration of 90 mg/L at different temperatures (as shown in Fig. 3) [26]. The applicability of the above two models can be determined from each linear plot of $\ln(q_e-q_t)$ against for pseudo-first-order, and t/q_t against for pseudo-second-order at 25°C, 35°C and 45°C, respectively. The results of the two models are presented in Fig. 6. Key parameter values of these two models calculated based on the slopes and increments of fitting curves in Figure (a) and (b) were listed in Table 1. The validity of each model was checked

Table 1: Parameters of the pseudo-first-order and pseudo-second-order for the adsorption of Pb(II) ions by MB
from an initial concentration of 90mg/L at 25℃, 35℃, 45℃.

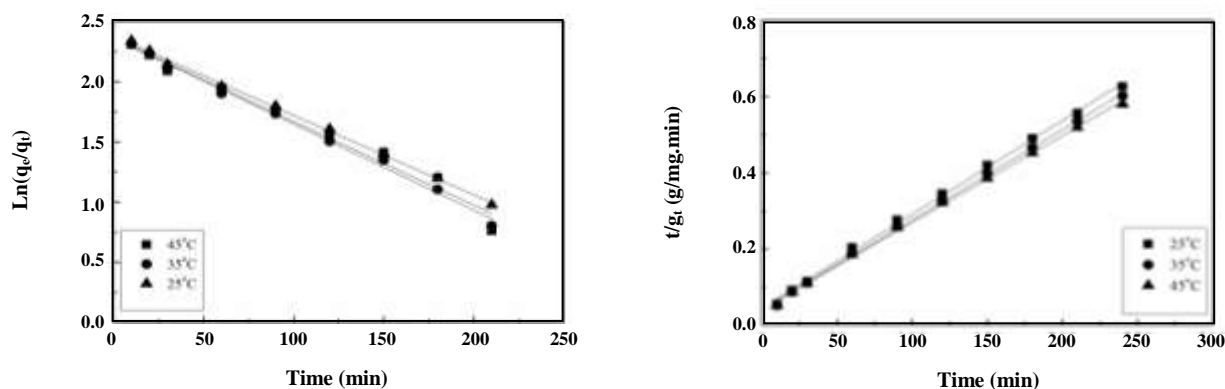| Temperatures (℃)	Experimental q_e (mg/g)	Pseudo-first-order			Pseudo-second-order		
		q_e (mg/g)	k_1 (min^{-1})	R^2	q_e (mg/g)	k_2 (g/mg·min)	R^2
25	380.23	292.78	0.0070	0.9767	377.36	0.0025	0.9981
35	399.24	296.58	0.0072	0.9942	400.00	0.0013	0.9990
45	414.11	310.60	0.0066	0.9977	434.78	0.0012	0.9984

Fig. 6: (a) Pseudo-first-order and (b) pseudo-second-order kinetics of the uptake of Pb(II) ions by MB.

using the coefficient of determination (R^2) calculated with these plots. It can be found that the coefficient of determinations (R^2) modified with pseudo-first-order model was $0.977 \sim 0.998$ and that with the pseudo-second-order model were $0.998 \sim 0.999$. In addition, the maximum adsorption quantities calculated based on the pseudo-first- and pseudo-second-order models were $377.36 \sim 434.78$ mg/g and $292.78 \sim 310.60$ mg/g at $25 \sim 45°C$, respectively. Clearly, the values of q_e calculated with the pseudo-second-order model coincided better with the experimental data ($380.23 \sim 414.11$ mg/g). The results illustrated that the two models have good applicability for the experimental data, but the pseudo-second-order model fitted better. Therefore, it can be inferred that chemisorption is the rate-limiting mechanism for the adsorption [23].

Adsorption isotherms

To investigate the interaction mechanisms of Pb(II) ions onto the adsorbent, adsorption equilibrium data of MB in a series of Pb(II) solution with different concentrations at different temperatures were fitted

by Langmuir isotherm model and Freundlich isotherm model, respectively. Fig. 7(a) and 7(b) shows the results of the linear regression procedures by Langmuir isotherm and Freundlich isotherm, respectively, and the related parameters (q_e, K_L, R^2, K_F, and $1/n$) of these models calculated based on the slopes and intervals were listed in Table 2. Compared with the R^2 values ($0.9259 \sim 0.9959$) of the experimental data fitted with the Freundlich model, that with the Langmuir model was much higher ($0.9914 \sim 0.9999$). The results illustrated that the adsorption process of Pb(II) ions onto MB is more suitable for Langmuir isotherm. It could be inferred that the Pb(II) ions mainly adsorbed by MB in the form of monolayer coverage on the adsorbent surface and lattice sites on the surface almost have the adsorptive capacities. When the surface was saturation, the MB would obtain the maximum adsorption capacity. As shown in Table 1, the values of q_e calculated by the Langmuir model were $403.26 \sim 561.80$ mg/L, which were only $1.00 \sim 5.76\%$ higher than the experimental q_e. In addition, Fig. 7 also shows that the adsorption capacity of MB increased as the temperature increases.

Table 2: Langmuir and Freundlich of adsorption isotherms of MB at 30 ℃, 40 ℃, 50 ℃

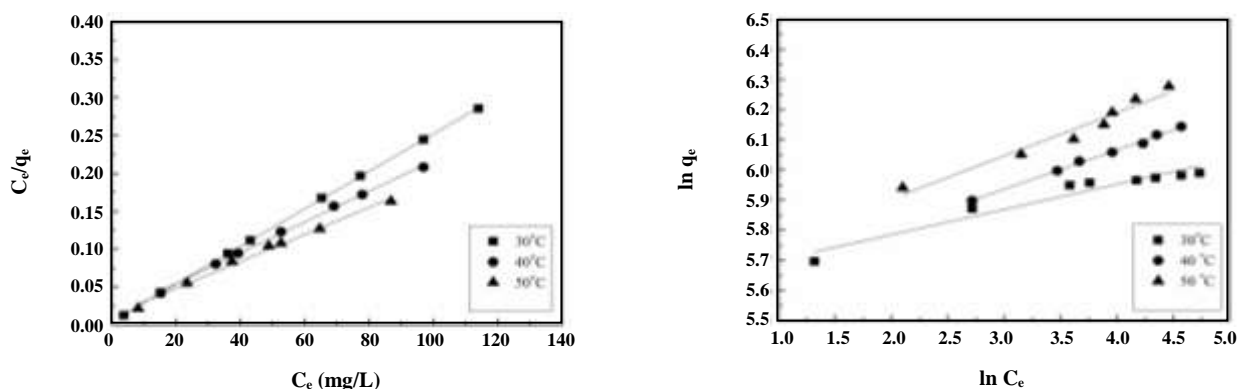| Temperatures (℃)	Experimental q_e (mg/g)	Langmuir			Freundlich		
		q_e (mg/g)	K_L (L/mg)	R^2	K_F	1/n	R^2
30	399.24	403.26	0.54	0.9999	275.31	0.0835	0.9259
40	465.78	492.61	0.15	0.9982	255.83	0.1303	0.9959
50	532.32	561.80	0.14	0.9914	275.37	0.1427	0.9489

Fig. 7: (a) Langmuir adsorption isotherm and (b) Freundlich adsorption isotherm of the uptake of Pb(II) ions by MB.

CONCLUSIONS

The adsorption performance of Pb(II) ions was investigated using modified biochar prepared with sewage sludge. It was concluded that MB was an effective adsorbent for Pb(II) removal from aqueous solution, the maximum adsorption capacity of Pb(II) was up to 380～414 mg/g for an initial Pb(II) concentration of 90 mg/L when pH=6. FTIR spectrum showed that principal functional groups took part in the adsorption process included carboxyl, hydroxyl and amino groups. The adsorption followed the pseudo-second-order kinetics equation which agrees with chemical adsorption being the rate controlling step. The experimental data obtained at different temperatures fitted with the Langmuir isotherm well, indicating the uptake capacity is monolayer adsorption. It may be also concluded that MB can be successfully used as a low-cost environment-friendly sorbent for the removal of contaminated water containing Pb(II) ions.

REFERENCES

[1] Shi Z., Zou P., Guo M., Yao S., Adsorption Equilibrium and Kinetics of Lead Ion onto Synthetic Ferrihydrites, *Iran. J. Chem. Chem. Eng. (IJCCE)*, **34**(3): 25-32 (2015).

[2] Blázquez G., Martín-Lara M.A., Tenorio G., Calero M., Batch Biosorption of Lead(II) from Aqueous Solutions by Olive Tree Pruning Waste: Equilibrium, Kinetics and Thermodynamic Study, *Chem. Eng. J.*, **168**(1), 170 (2011).

[3] Huang K., Zhu H., Removal of Pb^{2+} from Aqueous Solution by Adsorption on Chemically Modified Muskmelon Peel, *Environ. Sci. Pollut. Res.*, **20**(7): 4424-4434 (2017).

[4] Li Y.H., Di Z., Ding J., Wu D., Luan Z., Zhu Y., Adsorption Thermodynamic, Kinetic and Desorption Studies of Pb^{2+} on Carbon Nanotubes, *Water Res.,* **39**(4): 605-609 (2005).

[5] Shakeri A., Hazeri N., Valizadeh J., Hashemi E., Kakhky A.R.M., Removal of Lead (II) from Aqueous Solution Using Cocopeat: An Investigation on the Isotherm and Kinetic, *Iran. J. Chem. Chem. Eng. (IJCCE),* **31**(3): 45-50 (2012).

Research Article

[6] Kratochvil D., Volesky B., Advances in the Biosorption of Heavy Metals, *Trends in Biotechnology*, **16**(7): 291-300 (1998).

[7] Bailey S.E., Olin T.J., Bricka R.M., Adrian D.D., A Review of Potentially Low-Cost Sorbents for Heavy Metals, *Water Res.*, **33**(11): 2469-2479 (1999).

[8] Yousef R.I., El-Eswed B., Al-Muhtaseb A.H., Adsorption Characteristics of Natural Zeolites as Solid Adsorbents for Phenol Removal from Aqueous Solutions: Kinetics, Mechanism, and Thermodynamics Studies, *Chem. Eng. J.*, **171**(3): 1143-1149 (2011).

[9] Nekoo S.H., Shohreh F., Experimental Study and Adsorption Modeling of COD Reduction by Activated Carbon for Wastewater Treatment of Oil Refinery, *Iran. J. Chem. Chem. Eng. (IJCCE)*, **3**(32):81-89 (2013).

[10] Muftan H.E.-N., Sulaiman A.-Z., Alhaji M., Reduction of COD in Refinery Wastewater Through Adsorption on Date-pit Activated Carbon, *J. Hazard. Mater.*, **13**(1-3):750-757 (2010).

[11] Yang Y., Sheng G., Enhanced Pesticide Sorption by Soils Containing Particulate Matter from Crop Residue Burns, *Environ. Sci. Technol.*, **37**(16), 3635-3639 (2003).

[12] Zhu D., Kwon S., Pignatello, J.J., Adsorption of Single-Ring Organic Compounds to Wood Charcoals Prepared under Different Thermochemical Conditions, *Environ. Sci. Technol.*, **39**(11), 3990-3998 (2005).

[13] Wang X., Sato T., Xing B., Competitive Sorption of Pyrene on Wood Chars, *Environ. Sci. Technol.*, **40**(10), 3267-3272 (2006).

[14] Yu X., Pan L., Ying G., Kookana R.S., Enhanced and Irreversible Sorption of Pesticide Pyrimethanil by Soil Amended with Biochars, *J. Environ. Sci.*, **22**(4), 615-620 (2010).

[15] Chen D.Z., Zhang J.X., Chen J.M., Adsorption of Methyl Tert-butyl Ether Using Granular Activated Carbon: Equilibrium and Kinetic Analysis, *Int. J. Env. Sci. Tech.*, **7**(2):235-242 (2010).

[16] Wu Z., Li S., Wan J., Wang Y., Cr(VI) Adsorption on an Improved Synthesised Cross-Linked Chitosan Resin, *J. Mol. Liq.*, **170**, 25-29 (2012).

[17] Yan H., Zhang W., Kan X., Dong L., Jiang Z., Li H., Yang H., Cheng R., Sorption of Methylene Blue by Carboxymethyl Cellulose and Reuse Process in a Secondary Sorption, *Colloids Surf., A.*, **380**(1-3): 143-151 (2011).

[18] Ho Y.S., McKay G., Sorption of Dye from Aqueous Solution by Peat, *Chem. Eng. J.*, **70**(2): 115-124 (1998).

[19] D'Arcy R.L., Watt I.C., 1970. Analysis of Sorption Isotherms of Non-Homogeneous Sorbents, *Trans. Faraday Soc.*, **66**: 1236-1245 (1970).

[20] Laus R., Costa T.G., Szpoganicz B., Fávere V.T., Adsorption and Desorption of Cu(II), Cd(II) and Pb(II) Ions Using Chitosan Crosslinked with Epichlorohydrin-Triphosphate as the Adsorbent, *J. Hazard. Mater.*, **183**(1-3): 233-241 (2010).

[21] Swiatkowski A., Pakula M., Biniak S., Walczyk M., Influence of the Surface Chemistry of Modified Activated Carbon on Its Electrochemical Behaviour in the Presence of Lead(II) Ions, *Carbon*, **42**(15): 3057-3069 (2004).

[22] Lodeiro P., Barriada J.L., Herrero R., Sastre de Vicente M.E., The Marine Macroalga Cystoseira Baccata as Biosorbent for Cadmium(II) and Lead(II) Removal: Kinetic and Equilibrium Studies, *Environ. Pollut.*, **142**(2): 264-273 (2006).

[23] Acharya J., Sahu J.N., Mohanty C.R., Meikap B.C, Removal of Lead(II) from Wastewater by Activated Carbon Developed from Tamarind Wood by Zinc Chloride Activation, *Chem. Eng. J.*, **149**(1-3): 249-262 (2009).

[24] Chen X., Chen G., Chen L., Chen Y., Lehmann J., McBride M.B., Hay A.G., Adsorption of Copper and Zinc by Biochars Produced from Pyrolysis of Hardwood and Corn Straw in Aqueous Solution, *Bioresour. Technol.*, **102**(19): 8877-8884 (2011).

[25] Chen S., Yue Q., Gao B., Xu X., Equilibrium and Kinetic Adsorption Study of the Adsorptive Removal of Cr(VI) Using Modified Wheat Residue, *J. Colloid Interface Sci.*, **349**(1): 256-264 (2010).

[26] Sheela T., Nayaka Y.A., Viswanatha R., Basavanna S., Venkatesha T.G., Kinetics and Thermodynamics Studies on the Adsorption of Zn(II), Cd(II) and Hg(II) From Aqueous Solution Using Zinc Oxide Nanoparticles, *Powder Technol.*, **217**: 163-170 (2012).